Investigation of Electron Bernstein Wave (EBW) Coupling and its Critical Dependence on EBW Collisional Loss in High-β, H-Mode ST Plasmas

S.J. Diem[1], G. Taylor[2], J.B. Caughman[1], P.C. Efthimion[2], H. Kugel[2], B.P. LeBlanc[2], C.K. Phillips[2], J. Preinhaelter[3], S.A. Sabbagh[4], J. Urban[3], J.B. Wilgen[1]

[1]Oak Ridge National Laboratory, Oak Ridge, TN, USA
[2]Princeton Plasma Physics Laboratory, Princeton, NJ, USA
[3]Czech Institute of Plasma Physics, Prague, Czech Republic
[4]Columbia University, New York, NY, USA

e-mail contact of main author: diemsj@ornl.gov

Abstract. High-β spherical tokamak (ST) plasma conditions cut off propagation of electron cyclotron (EC) waves used for heating and current drive in conventional aspect ratio tokamaks. The electron Bernstein wave (EBW) has no density cut off and is strongly absorbed and emitted at the EC harmonics, allowing EBWs to be used for heating and current in STs. However, this application requires efficient EBW coupling in the high-β, H-mode ST plasma regime. EBW emission (EBE) diagnostics and modelling have been employed on the National Spherical Torus Experiment (NSTX) to study oblique EBW to O-mode (B-X-O) coupling and propagation in H-mode plasmas. Efficient EBW coupling was measured before the L-H transition, but rapidly decayed thereafter. EBE simulations show EBW collisional damping prior to mode conversion (MC) in the plasma scrape off reduces the coupling efficiency during the H-mode phase when the electron temperature is less than 30 eV inside the MC layer. Lithium evaporation during H-mode plasmas was successfully used to reduce this EBW collisional damping by reducing the electron density and increase the electron temperature in the plasma scrape off. Lithium conditioning increased the measured B-X-O coupling efficiency from less than 10% to 60%, consistent with EBE simulations.

1. Introduction

Tokamaks and many other magnetically confined plasma devices have utilized electron cyclotron (EC) waves to provide local electron temperature, T_e, measurements via EC emission (ECE) [1] as well as for localized heating via electron cyclotron resonance heating (ECRH), and current drive via electron cyclotron current drive (ECCD) [2]. However, high-β devices, such as the spherical tokamak (ST) and reverse field pinch, routinely operate at relatively high electron densities, n_e, compared to the confining magnetic field, such that the plasmas are overdense, $\omega_{pe} \gg \Omega_{ce}$, where ω_{pe} is the electron plasma frequency and Ω_{ce} is the electron cyclotron frequency. In these overdense devices, propagation of EC waves beyond the plasma edge is cutoff, thus prohibiting the use of ECRH or ECCD. The National Spherical Torus Experiment (NSTX, [3]) routinely studies overdense plasmas with n_e up to 10^{20} m^{-3} and $B_t < 0.6$ T, so that the first four EC harmonics are overdense. An alternative to EC waves for these overdense devices is the electrostatic electron Bernstein wave (EBW) [4]. EBWs do not experience a density cutoff in the plasma, propagate mainly perpendicular to the external magnetic field and are strongly absorbed at and emitted from EC resonances. However, EBWs cannot propagate outside the plasma and therefore must couple to the ordinary (O) or extraordinary (X) electromagnetic modes outside the overdense region of the plasma. Coupling to the EBW can be achieved through B-X (EBW to X-mode coupling) or B-X-O (EBW to X-mode to O-mode coupling) mode conversion. The work presented here studied microwave plasma emission via B-X-O coupling on NSTX.

In the B-X-O emission process, an EBW is generated near the location where the wave frequency, ω, is equal to a harmonic of the Ω_{ce}. The EBW travels radially outward towards the plasma edge, perpendicular to the plasma magnetic field, until it encounters the upper hybrid resonance (UHR) layer where $\omega = \omega_{UHR} = ((\omega_{pe})^2 + (\Omega_{ce})^2)^{1/2}$. At this point, the perpendicular wave number, $k_\perp$, of the EBW and slow X-mode branch are equal and full conversion between the two branches occurs. The converted slow X-mode propagates back into the plasma until it encounters the left-hand cutoff of the X-mode. For particular viewing angles, the left-hand cutoff of the slow X-mode branch is coincident with the O-mode cutoff ($\omega = \omega_{pe}$) and the power in the slow X-mode can be transferred efficiently to the O-mode branch. The O-mode then propagates out of the plasma and can be detected by a receiving antenna with an oblique view of the plasma. The transmission window for this process is given by [5]:

$$T\left(n_{\parallel}, n_{\perp}\right) = \exp\left\{-\pi k_o L_n \sqrt{\frac{Y}{2}}\left[2(1+Y)\left(n_{\parallel,opt} - n_{\parallel}\right)^2 + n_y^2\right]\right\} \tag{1}$$

$$Y = \frac{\Omega_{ce}}{\omega} \tag{2}$$

$$n_{\parallel,opt}^2 = \frac{Y}{1+Y} \tag{3}$$

In equation (1) above, $n_{\parallel}$ and $n_{\perp}$ are the parallel and perpendicular wave numbers, respectively, k_o is the vacuum wavelength, and L_n is the density scale length evaluated at the mode conversion (MC) layer. L_n determines the angular width of the window. By decreasing L_n, the angular width of the window is increased. The center of the B-X-O transmission window in poloidal and toroidal angle depends on the magnetic field and its pitch angle at the MC layer. The B-X-O transmission efficiency in equation (1) only calculates the transmission at the O-mode cutoff layer and does not account for re-absorption and re-emission prior to conversion. An EBW emission (EBE) simulation code was used to calculate these losses.

The inverse process of O-X-B mode conversion can be used to inject power into the plasma to provide localized heating and current drive (CD). The physics of B-X-O emission and O-X-B injection are essentially the same except that the introduction of radiofrequency power may excite lossy nonlinear effects such as parametric decay. Therefore, studying B-X-O emission can be used to assess the feasibility of O-X-B coupling. Modeling has shown that adding 1 MA of off-axis EBW current drive (EBWCD) to an ST Component Test Facility (ST-CTF) plasma significantly increases plasma stability [6] and that efficient Ohkawa EBWCD can be driven well off axis [7]. However, a critical challenge for EBWCD for the ST-CTF is to establish and maintain efficient antenna coupling to the EBW in the plasma during High confinement (H-mode) operation.

This paper presents details of EBE measurements made via B-X-O coupling during NSTX H-mode plasmas. Section 2 describes the NSTX B-X-O emission diagnostic and the EBE simulation code used to model plasma emission. Section 3 presents the EBE measurements obtained during H-mode experiments. Early low emission results (Section 3.1) were determined to be caused by collisional damping of the EBW prior to mode conversion. Edge conditioning was employed to significantly increase the EBE levels (Section 3.2) allowing for an experimental mapping of the B-X-O transmission window to be performed (Section 3.3). Section 4 summarizes the conclusions.

2. Experimental Setup and EBE Simulation

The EBE diagnostic on NSTX consists of two remotely-steered, quadridged microwave antennas [8, 9]. The antennas are located outside of the vacuum vessel, 50 cm from the plasma edge, and have an oblique view of the plasma so the diagnostic is optimized to measure B-X-O emission. The quadridged antennas allow for a simultaneous measurement of the radiation temperature, T_{rad}, parallel (O-mode component) and perpendicular (X-mode component) to the plasma's magnetic field when the magnetic field pitch at the MC layer is between 30° and 45°. The ratio of parallel to perpendicular components yields the polarization of the incoming radiation while the sum provides the total T_{rad}. The system measures fundamental, second and third harmonic emission ranging from 8-36 GHz. Each antenna mount has two linear actuators that provide movement in the poloidal and toroidal directions between discharges, this feature allows for detailed measurements of the B-X-O transmission window. Each antenna is coupled to a dual-channel, absolutely calibrated, heterodyne radiometer system. The local oscillator for each radiometer is swept at a rate of 10 kHz to provide emission profile measurements. Results presented in this paper are from the 18-36 GHz frequency range. The optical depth for EBWs at low EC harmonic resonances is ~ 3000 in NSTX [10], well satisfying the blackbody condition of $\tau > 2$, so the measured T_{rad} can be assumed to be equal to the local T_e provided the B-X-O transmission efficiency is ~ 100%. For cases such that the transmission is less than 100%, EBE simulations were used to deduce the transmission efficiency.

The EBE measurements were simulated with a numerical code developed by Preinhaelter et al. [11]. The code simulates the process of O-X-B injection; however, due to the reciprocity of the injection and emission processes [12], the absorption and emission locations are assumed to be equivalent. A bundle of 41 rays is launched in the code to simulate the measured antenna pattern of the EBE diagnostic. A full-wave code [13] calculates the transmission efficiency of the O-X-B mode conversion assuming a 1-D plasma slab model. A 3-D ray-tracing code calculates the propagation and absorption of the EBW after it has mode converted. The inputs for the EBE code are the T_e and n_e profiles measured by laser Thomson scattering [14] and the magnetic equilibrium reconstructed by EFIT [15]. Collisions between electrons and ions are incorporated into the EBE code with a Bhatnagar-Krook-Gross collision operator [16, 17]. The simulations neglect the effects of electron-electron collisions due to conservation of momentum while electron-neutral collisions are discarded because the neutral density is less than 5% of the n_e in the vicinity of the MC layer in NSTX plasmas.

3. Experimental Results

Good O-X-B coupling in H-mode plasmas is especially important for future STs that will routinely operate in in this regime and require localized EBWCD or EBW heating (EBWH) to maintain stability at high β. Recent EBE measurements on NSTX have investigated B-X-O coupling in H-mode plasmas to assess the feasibility of establishing efficient EBW coupling.

3.1. Low H-mode EBE results

Early EBE measurements in NSTX H-mode plasmas revealed very low B-X-O transmission efficiencies of less than 10% during the plasma current flattop. The characteristics of a typical H-mode plasma in NSTX, with I_p of 1 MA and central n_e and T_e of $4\text{-}6\text{x}10^{13}$ cm^{-3} and 0.9 keV, respectively, are shown in figure 1. For these H-mode discharges, the measured B-X-O transmission efficiencies were 20-60% for f_{ce}, $2f_{ce}$ and $3f_{ce}$ (18-36 GHz) emission during the

L-H transition. However, during the H-mode phase the measured T_{rad} was less than 10 eV for all measured harmonics. The emission location for second harmonic (24 GHz) emission (figure 1) remained at a constant major radius of 1 m, near the plasma magnetic axis, throughout the discharge.
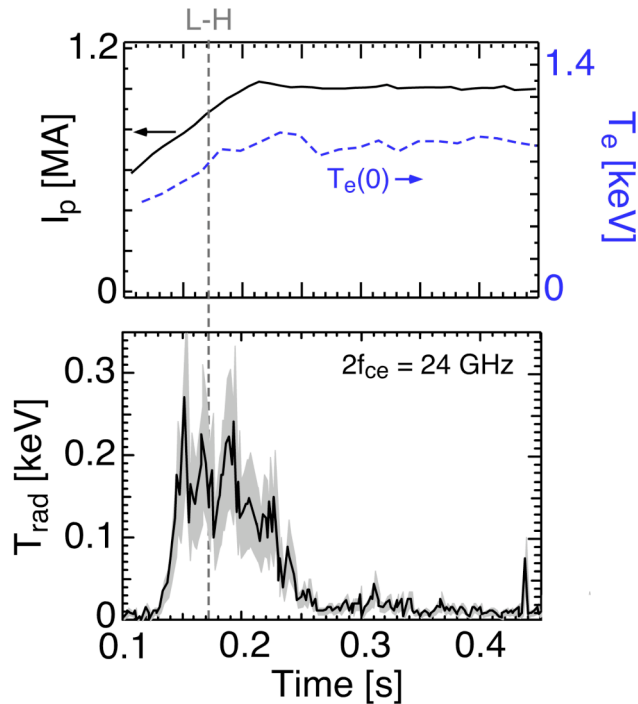

FIG. 1. (top) The I_p (solid line) and central T_e (dashed line) are shown as a function of time for an H-mode discharge. (bottom) The time evolution of second harmonic emission at 24 GHz, from near the plasma magnetic axis, is shown for an H-mode discharge. The shaded region represents the uncertainty in the measured T_{rad}.

Preinhaelter et al. [11] suggested that the observed decay in EBE could be explained by collisional damping of the EBW prior to mode-conversion to the slow X-mode. Modeling suggests EBW collisional damping becomes significant if the electron-ion collision frequency, υ_{ei}, is greater than $10^{-4}\omega$, which typically corresponds to $T_e < 20$ at the MC layer for NSTX plasmas. For times prior to t = 0.25 s for the discharge shown in figure 1, the B-X-O MC layer is located within 1 cm of the last closed flux surface (LCFS) as seen in figure 2. For times greater than 0.25 s, the MC layer is shifted 3 to 9 centimeters outside of the LCFS where T_e is lower than 10 eV (figure 2). EBE simulations of this plasma without incorporating any effects of collisional damping prior to MC (top solid line in figure 3) predict $T_{rad} \sim 0.8$ keV, significantly higher than the measured T_{rad} (bottom solid line in figure 2) which was < 20 eV. By including EBW collisional damping prior to MC in the EBE simulations and the measured Z_{eff} from the CHarge Exchange and Recombination Spectroscopy (CHERS) diagnostic on NSTX [18] the simulations predict the rapid decay in T_{rad} observed in the experiment (dashed line in figure 3), but they do not reproduce the observed low T_{rad} values.
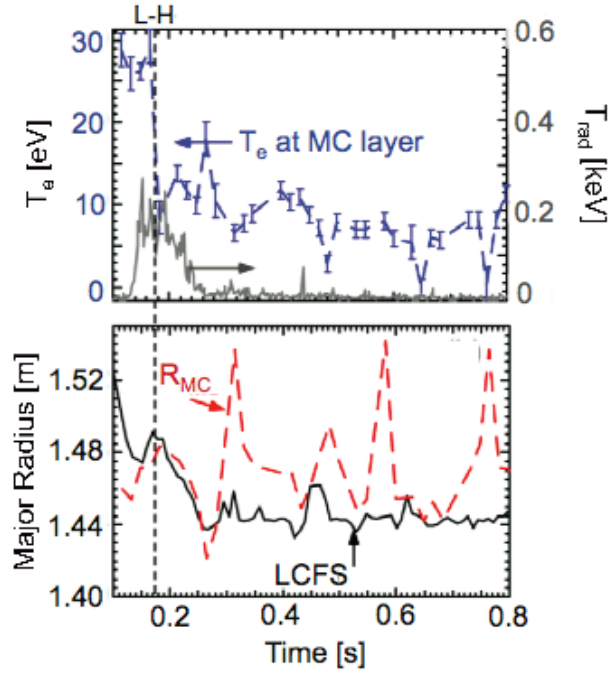
FIG. 2. (top) The time evolution of T_e at the MC layer (dashed line) and the measured radiation temperature, T_{rad}, (solid line) are shown. The vertical error bars represent the error in the Thomson scattering measurements. (bottom) The time evolution of the location of the last closed flux surface (solid line) and the position of the mode conversion layer, R_{MC}, (dashed line) are shown. The vertical dashed line indicates the L-H transition time.

In the simulation shown in figure 3, a Z_{eff} value of 2 was used. This value was the closest Z_{eff} measurement available from the CHERS (located 5 cm inboard from the MC layer). The Z_{eff} measurement from CHERS is calculated based upon the line emission from plasmas where the sole impurity is assumed to be carbon. For many of these plasmas, other impurities are present. EBE simulations with Z_{eff} of 3-4 predict T_{rad} levels during the H-mode phase that agree more closely with the measured results (figure 4).
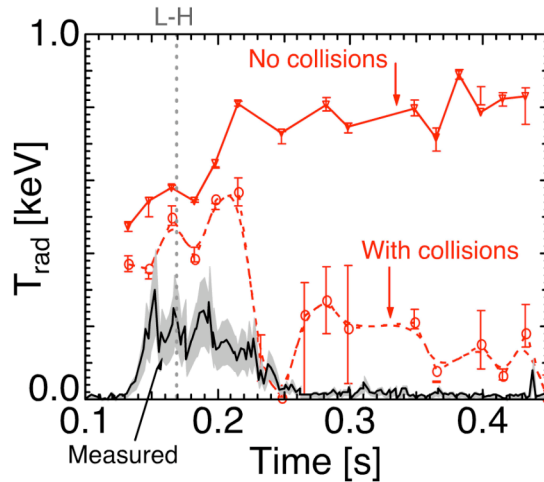

FIG. 3. EBE simulations of the low emission H-mode data, with (dashed line) and without (solid line) collisional damping effects. The error bars represent the uncertainty in the simulations due to errors in n_e and T_e from Thomson scattering as well as the magnetic equilibrium reconstruction.
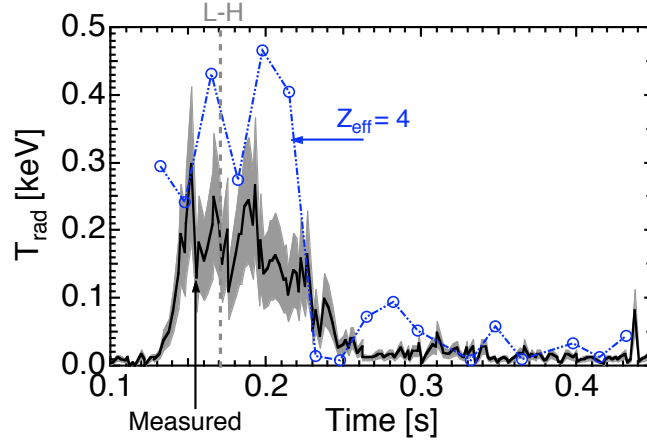
5

FIG. 4. *EBE simulations of the low emission H-mode data with collisional effects, assuming $Z_{eff} = 4$.*

The EBE simulation calculates that the ratio of υ_{ei}/ω near the mode conversion layer increased over a factor of 2 from 5×10^{-5} at t = 0.148 s to 1.25×10^{-4} at t = 0.348 s. The value of υ_{ei}/ω after the L-H transition exceeded the simulated threshold of $\upsilon_{ei}/\omega > 10^{-4}$ for significant damping. Nearly 20-40% of the ray intensity is collisionally damped prior to the L-H transition compared to 70-90% after the transition.

The results of these early H-mode experiments and simulations suggest that by decreasing the collisionality at the MC layer, significant improvements in the power coupled from the EBW to slow X-mode branch may be achieved. Since $\upsilon_{ei} \propto n_e T_e^{-1/2}$, either the density can be decreased or T_e increased to reduce collisional effects in the plasma edge. This motivated the need for an edge conditioning tool to decrease n_e outside the LCFS, which results in shifting the MC layer to a warmer region of the plasma. The next section discusses the method employed for edge conditioning and the resulting effects on the EBE levels.

3.2 H-mode EBE results with lithium conditioning

Edge conditioning using lithium (Li) coatings on the plasma facing components has been achieved with a Li evaporation oven (LITER) [19] installed on an upper vacuum vessel port in NSTX. LITER evaporates Li onto the graphite tiles of the centerstack and lower divertor before and during a discharge. The solid Li coating pumps D^+ and D^o by forming LiD. During a series of EBE experiments to enhance EBW coupling in H-mode discharges, the Li evaporation rate was varied from 0 to 19 mg/min to observe the effect on the EBE T_{rad} levels. The time evolution of major plasma parameters for the target H-mode discharge used in this study are shown in figure 5. As a result of Li edge conditioning, n_e in the plasma scrape off was reduced by nearly a factor of two and consequently the MC layer moved from several centimeters outside the LCFS to the plasma separatrix (figure 6). By moving the MC layer closer to the plasma, T_e at the fundamental MC layer during the H-mode phase increased from 5-9 eV (no Li) to nearly 20 eV (with 19 mg/min of evaporated Li) as shown in figure 7.
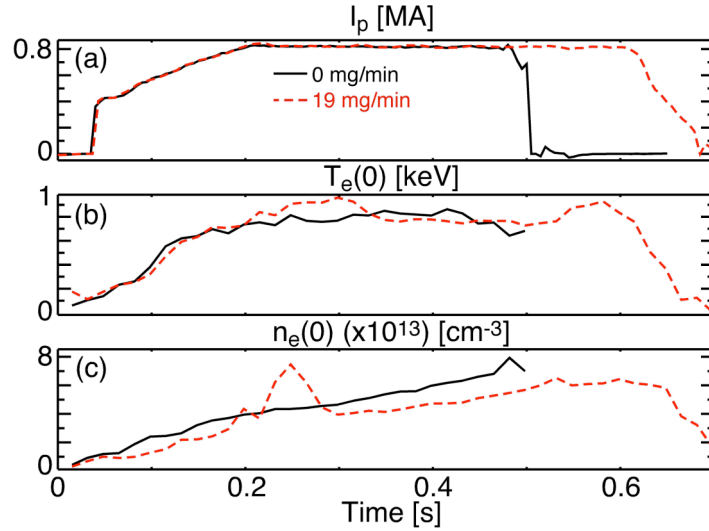
6

FIG. 5. The time evolution of (a) I_p, (b) $T_e(0)$, and (c) $n_e(0)$ are shown for the target H-mode plasmas for the cases with 0 (solid line, no Li) and 19 mg/min (dashed line) of evaporated Li. The L-H transition occurs at 0.145 s.
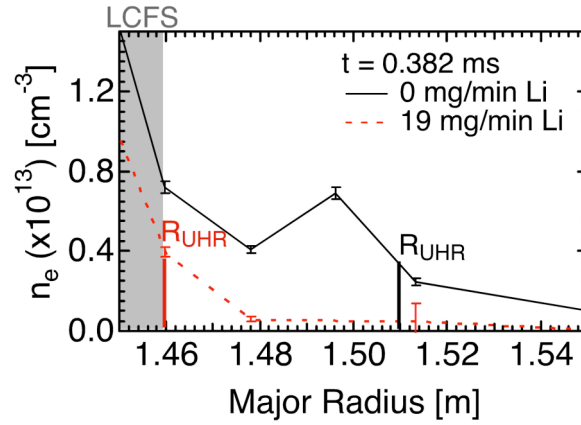

FIG. 6. The n_e profile from Thomson scattering is shown as a function of major radius in the plasma scrape off for two cases: no evaporated Li (solid line) and with 19 mg/min of evaporated Li (dashed line).
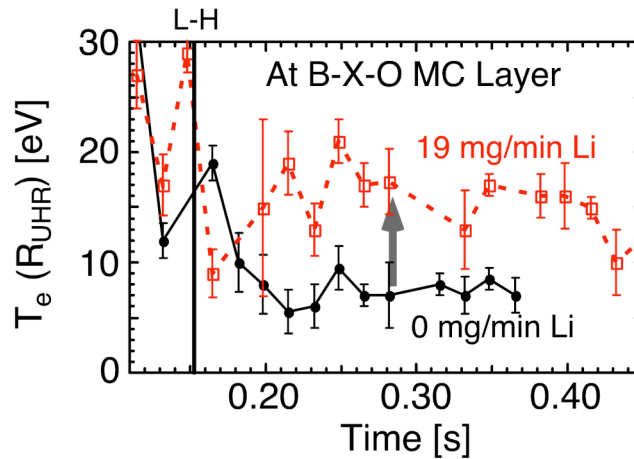

FIG. 7. The time evolution of T_e, measured by laser Thomson scattering, at the MC layer (where $\omega = \omega_{UHR}$) is shown for a plasma without Li conditioning (solid line) and with Li conditioning (dashed line). The solid vertical line indicates the L-H transition while the vertical error bars represent the uncertainty in the Thomson scattering measurement.
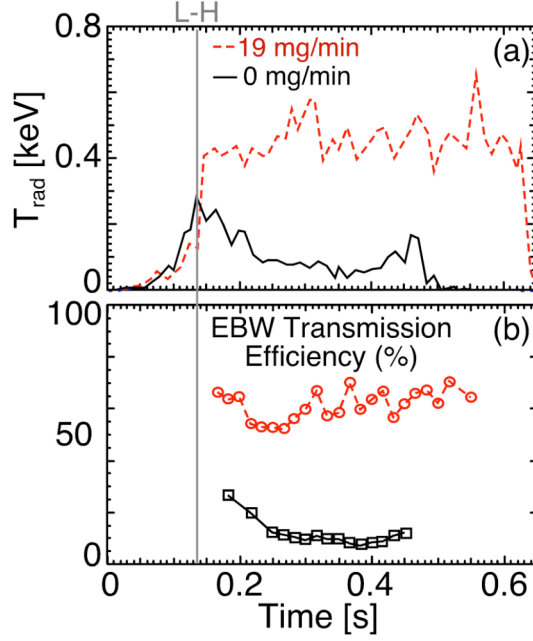
7

FIG. 8. (a) The measured T_{rad} and (b) B-X-O transmission efficiency are plotted for fundamental EBE (at 18 GHz) for Li evaporation rates of 0 mg/min (solid line) and 19 mg/min (dashed line).

A significant increase in the measured T_{rad} from less than 50 eV to greater than 450 eV for f_{ce} = 18GHz (near axis emission) was observed (figure 8 (a)) and agreed with the EBE simulated T_{rad}. The measured B-X-O transmission efficiency was observed to increase from less than 10% (no Li) to 60% (with Li) as shown in figure 8 (b). Additionally, υ_{ei}/ω near the mode conversion layer decreased by a factor of three from 1.2×10^{-4} (no Li) to 4×10^{-5} (with Li) as seen in figure 9. Consequently, the EBW ray intensity lost to collisional damping (figure 9) was reduced from 70% (no Li) to only 15% (with Li).
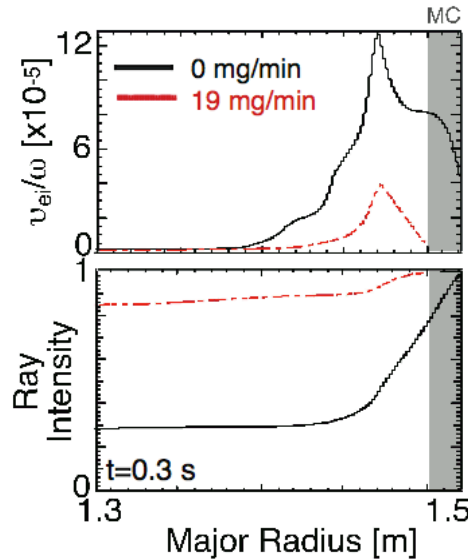

FIG. 9. The ratio of υ_{ei}/ω (top) and the intensity of the central ray (bottom) from the EBE simulation of a plasma without Li conditioning (solid line) and one with Li conditioning (dashed line) are shown as a function of major radius. The shaded region indicated the location of the MC layer.

The use of Li edge conditioning to increase the B-X-O transmission efficiency allowed for the development of a suitable target plasma to map the angular dependence of the B-X-O

8

transmission efficiency window (equation 1). The next section presents the experimental results from a mapping of the B-X-O transmission window obtained by scanning the EBW antenna viewing direction in the poloidal and toroidal directions.

3.3 Experimental mapping of the B-X-O transmission window

A series of target H-mode discharges, with an I_p = 0.9 MA, $T_e(0)$ ~ 0.8-0.9 keV, and $n_e(0)$ ~ 3-5x10^{13} cm^{-3}, were used for mapping the B-X-O transmission efficiency window. Li was continuously evaporated at a rate of 17 mg/min during each discharge to reduce collisional losses to less than 20%, as indicated by EBE simulations. The target plasma was repeated and the EBE diagnostic antenna was steered to a new viewing direction between discharges. The measured and predicted B-X-O transmission efficiency maps for fundamental (18 GHz) and second harmonic (28 GHz), near axis emission, are shown in figure 10. The maximum measured B-X-O transmission efficiency was 62±15% for fundamental and 48±15% for second harmonic emission. Good agreement, less than 5°, between the measured and theoretical locations (equation 1) of the optimum angles was observed. The EBE simulation code was used to determine the poloidal and toroidal angles for optimal transmission, these angles were also within 5° of the measured value. The predicted angle location for optimal EBW transmission from both the theoretical calculations and the EBE simulations are within the 14° acceptance angle of the antenna.
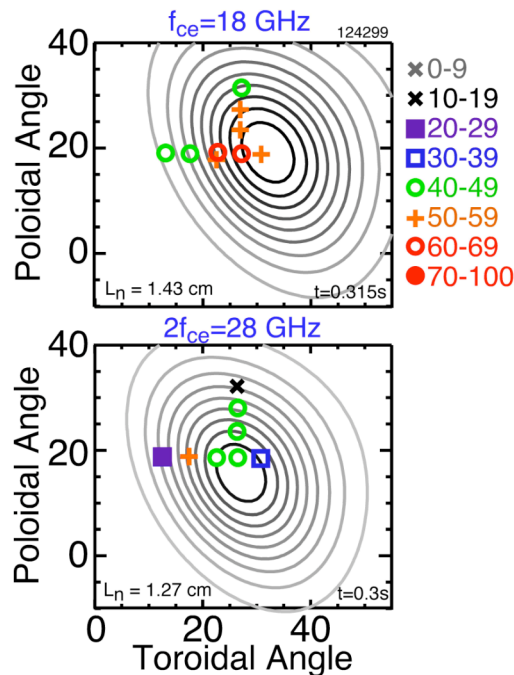

FIG. 10. Experimentally measured B-X-O transmission efficiency map (symbols) in a Li conditioned H-mode plasma for (a) f_{ce} = 18 GHz and (b) $2f_{ce}$ = 28 GHz. The contours represent the theoretical B-X-O transmission efficiency (equation 1), where the center represents 90% transmission. Subsequent contours represent a 10% decrease in transmission.

4. Conclusion

Early H-mode experiments revealed very low B-X-O transmission efficiencies, with less than 10% transmission being observed during the I_p flattop for the 18-36 GHz EBE frequency range measured. Simulations of these H-mode discharges suggested that the low emission

results from significant collisional damping of the EBW prior to mode conversion. These results motivated the need for a tool to reduce the edge collisionality in these plasmas. Lithium evaporation was used to deplete n_e in the plasma scrape off, moving the MC layer to a region in the plasma where $T_e \sim 20$ eV. At these temperatures, the collisionality near the MC layer is significantly reduced, which increased the fundamental B-X-O transmission efficiency from 10% to 60%, agreeing with EBE simulation results. Similarly, the second harmonic B-X-O transmission efficiency was increased from 25% to 50%. The increase in EBE during H-mode allowed for an experimental mapping of the B-X-O transmission efficiency to be obtained. The measured, theoretically predicted (equation 1), and simulated optimum toroidal and poloidal angles for maximum transmission in H-mode plasmas agreed within 5°, verifying that these tools can be used to determine the optimal launch angle and polarization for future EBW heating and CD systems. This work has demonstrated that using edge conditioning to raise T_e at the MC layer can significantly reduce collisional losses, providing support for EBW as a viable candidate for localized heating and CD in future ST devices.

Acknowledgements

References

[1] TAYLOR, G., Fus. Sci. Tech. **52** (2007), 119.
[2] ZOHM, H., Fus. Sci. Tech. **52** (2007), 134.
[3] ONO, M., et al., Nucl. Fusion **40** (2000) 557.
[4] BERNSTEIN, I.B., Phys. Rev. **109** (1958) 10.
[5] MJØLHUS, E., J. Plasma Phys. **31** (1984) 7.
[6] PENG, Y-K. M, Plasma Phys. Control. Fusion **47** (2005) B263.
[7] TAYLOR, G., et al., Phys. Plasmas **11**, (2004) 4733.
[8] DIEM, S.J., et al., Rev. Sci. Instrum. **77** (2006) 10E919.
[9] DIEM, S.J., et al., Rev. Sci. Instrum. 79 (2008) 10F101.
[10] EFTHIMION, P.C., et al., Rev. Sci. Instrum. **70** (1999) 1018.
[11] PREINHAELTER, J., et al., Rev. Sci. Instrum. **77** (2006) 10F524.
[12] RAM, A.K., BERS, A., and LASHMORE, C.N., Phys. Plasmas **9** (2002) 409.
[13] URBAN, J. and PREINHAELTER, J., J. Plasma Phys. **72** (2006) 1041.
[14] LEBLANC, B. P., et al., Rev. Sci. Instrum. **74** (2003) 1659.
[15] LAO, L., et al., Nucl. Fusion **25** (1985) 1611.
[16] BHATNAGAR, P.L., GROSS, E.P., and KROOK, M., Phys. Rev. **94** (1954) 511.
[17] GROSS, E.P. and KROOK, M., Phys. Rev. **102** (1956) 593.
[18] BELL, R. E., et al., "Z_{eff} Profiles using Charge Exchange Recombination Spectroscopy on NSTX", Bull. Am. Phys. Society **48 (7)** (2003).
[19] KUGEL, H.W., et al., Journal of Nuc. Mater. **363-365** (2007) 791.